

Downlink Performance Analysis for a Generalized Shotgun Cellular System

Prasanna Madhusudhanan*, Juan G. Restrepo[†], Youjian (Eugene) Liu*, Timothy X Brown^{*+},
and Kenneth Baker⁺

*Department of Electrical, Computer and Energy Engineering,

[†]Department of Applied Mathematics, ⁺Interdisciplinary Telecommunications Program

University of Colorado, Boulder, CO 80309-0425 USA

{mprasanna, juanga, eugeneliu, timxb, kenneth.baker}@colorado.edu

Abstract

In this paper, we analyze the signal-to-interference-plus-noise ratio (SINR) performance at a mobile station (MS) in a random cellular network. The cellular network is formed by base-stations (BSs) placed in a one, two or three dimensional space according to a possibly non-homogeneous Poisson point process, which is a generalization of the so-called shotgun cellular system. We develop a sequence of equivalence relations for the SCSs and use them to derive semi-analytical expressions for the coverage probability at the MS when the transmissions from each BS may be affected by random fading with arbitrary distributions as well as attenuation following arbitrary path-loss models. For homogeneous Poisson point processes in the interference-limited case with power-law path-loss model, we show that the SINR distribution is the same for all fading distributions and is not a function of the base station density. In addition, the influence of random transmission powers, power control, multiple channel reuse groups on the downlink performance are also discussed. The techniques developed for the analysis of SINR have applications beyond cellular networks and can be used in similar studies for cognitive radio networks, femtocell networks and other heterogeneous and multi-tier networks.

Index Terms

Cellular Radio, Co-channel Interference, Random Cellular Deployments, Fading Channels, Stochastic Ordering.

I. INTRODUCTION

The modern cellular communication network is a complex overlay of heterogeneous networks such as macrocells, microcells, picocells, and femtocells. The base station (BS) deployment for these network can be planned, unplanned, or uncoordinated. Even when planned, the base station (BS) placement in a region typically deviates from the ideal regular hexagonal grid due to site-acquisition difficulties, variable traffic load, and terrain. The coexistence of heterogeneous networks has further added to these deviations. As a result, the BS distribution appears increasingly irregular as the BS density grows and is outside standard performance analysis.

Two approaches of modeling have been widely adopted in the literature. At one end, the BSs are located at the centers of regular hexagonal cells to form an ideal hexagonal cellular system. At the other end, the BS deployments are modeled according to a Poisson point process which we refer to as shotgun cellular system (SCS). In [1], we make a connection between these two models on a homogeneous two dimensional (2-D) plane. It is shown that the signal-to-interference ratio, (SIR), of the SCS lower bounds that of the ideal hexagonal cellular system and, moreover, the two models converge in the strong fading regime. Since the BS deployment in the practical cellular system lies somewhere in between these two extremes, the analysis of SCSs is important to completely understand the performance of the cellular networks. Such an analysis holds significance in areas beyond cellular networks. Wireless LANs, cognitive radios, and ad-hoc networks are also characterized by irregular deployment of the BSs [2]–[18]. It is emphasized that, although the deployment of BSs in practice is not random, such a study is useful because it allows a thorough theoretical understanding of many important effects in the strong fading regime.

A Poisson point process has been adopted in the literature for the locations of nodes in the study of sensor networks, ad hoc networks and other uncoordinated and decentralized networks. In the case of ad-hoc networks, bounds on the transmission capacity have been derived in several different contexts [7], [8], [11]–[13], [19]–[22]. Finding the optimal bandwidth partitioning in uncoordinated wireless networks is considered in [23]. Similar outage probability analysis in ad-hoc packet radio networks is considered in [24], [25].

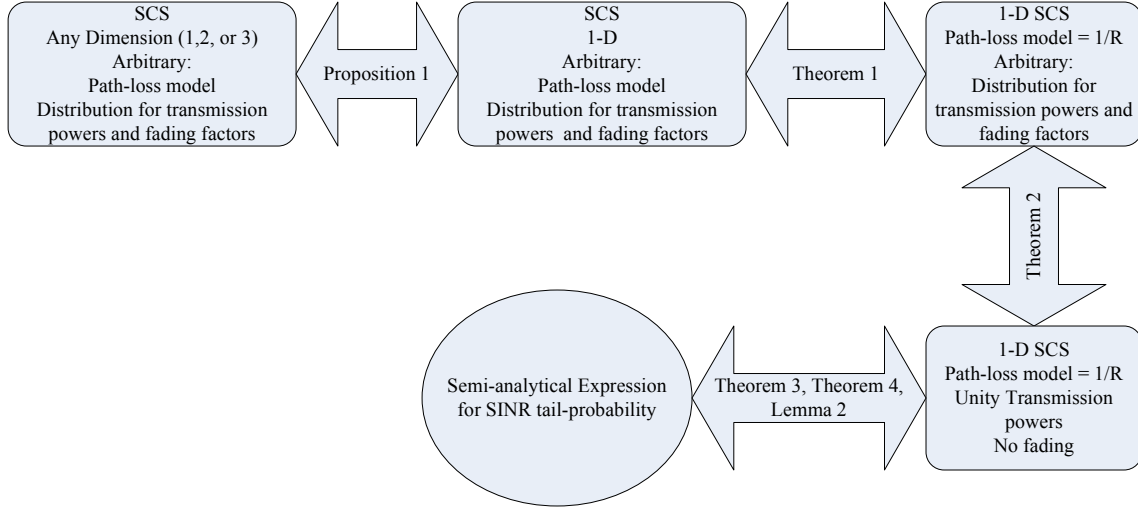


Figure 1: Contributions of this paper: SINR characterization for 1-D SCSs

An underlying assumption in all the previous work is that the density of transmitters is constant throughout the cellular region, i.e. the Poisson point process is homogeneous. Such a model does not appropriately represent practical cellular networks where the BS distribution is irregular. In this paper, this scenario is incorporated by modeling the distribution of BSs by a non-homogeneous Poisson point process. Moreover, the region of interest need not be restricted to \mathbb{R}^2 as in prior work, and may be \mathbb{R}^1 or \mathbb{R}^3 . Furthermore, the performance dependence on the MS location within the non-homogeneous cellular region is also characterized. Handoff features and other dynamics are out of the scope of this work.

Finally, most research restricts the interference analysis to popular fading models like log-normal, Rayleigh, and Rician distributions and a propagation model that follows the power law path-loss. Here, the results hold for arbitrary fading distribution and arbitrary path-loss models. This helps in more accurately modeling the wireless network.

The main contributions of this paper are depicted in Figures 1 and 2. For general system model where the BS arrangement is according to a non-homogeneous Poisson point process in an arbitrary dimension ($l = 1, 2, 3$), for arbitrary path-loss models and arbitrary distributions of the independent and identically distributed (i.i.d.) random transmission powers and fading factors, we successively reduce the actual system to a canonical model that is equivalent in terms of the

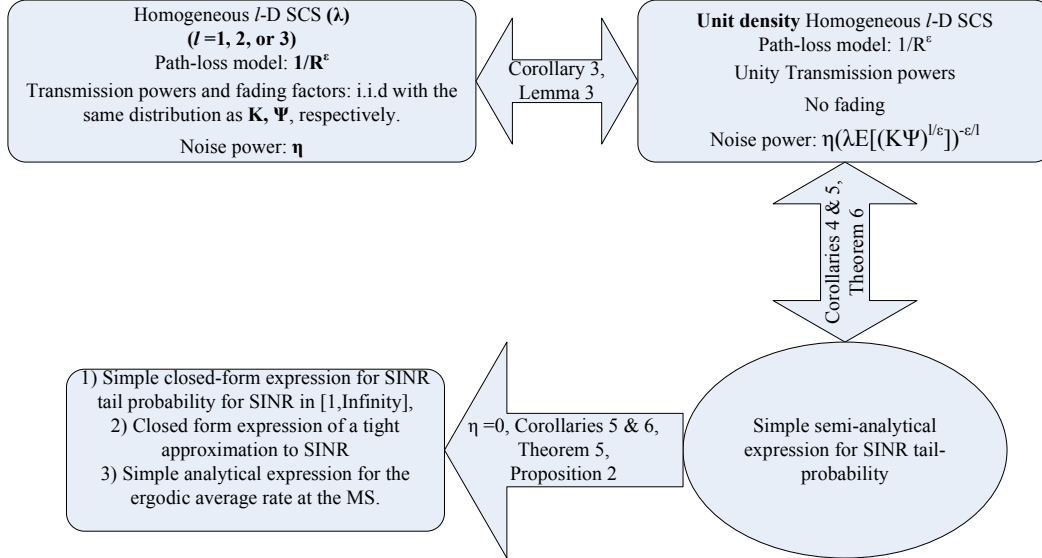


Figure 2: Contributions of this paper: SINR characterization for homogeneous l -D SCSs

SINR characteristics, and characterize the SINR distribution for the simplest equivalent system, thereby solving the problem for the most general network. For the case of homogeneous SCSs, which is the most widely used model for random node locations, we obtain simple closed form characterizations of the SINR, as well as several insight about the network. This is briefly shown in Figure 2.

Applications of the above results in specific wireless communication scenarios are briefly described in Section VI followed by the conclusions. Next, the system model and the performance metric of interest are briefly explained.

II. SYSTEM MODEL

This section describes the various elements used to model the shotgun cellular system, namely, the BS layout, the radio environment, and the performance metrics of interest.

A. BS Layout

Definition 1. The *Shotgun Cellular System (SCS)* is a model for the cellular system in which the BSs are placed in a given l -dimensional plane (typically $l = 1, 2$, and 3) according to a non-homogeneous Poisson point process on \mathbb{R}^l [26], [27].

The intensity function of the Poisson point process is called the BS density function in the context of the SCS. A 1-D SCS models, for example, the BS deployments along a highway. A 2-D SCS models planar BS deployments, and the 3-D SCS models BS deployments in a dense urban area, or wireless LANs in an apartment building. The 1-D, 2-D and 3-D SCSs are described using the BS density functions $d(x)$, $d(r, \theta)$, and $d(r, \theta, \phi)$, where $-\infty \leq x \leq \infty$ represents a point in 1-D, and r , θ , ϕ are used to represent a point in polar coordinates, in 2-D and 3-D.

A l -D SCS is said to be homogeneous if the BS density function is a constant over the entire l -D space. A homogeneous 2-D SCS is a common model for the random node placement in many scenarios.

We consider the most general possible description for the wireless radio environment. Let the received power at a distance r (≥ 0) from a given BS be given by

$$P(r) = K\Psi/h(r), \quad (1)$$

where K represents the transmission power and the antenna gain of the BS, Ψ captures the channel gain, and the function $h(\cdot)$ represents a path-loss that a signal experiences as it propagates in the wireless environment. The most commonly used path-loss model is the power-law path-loss model, $h(r) = r^\varepsilon$, where ε is called the path-loss exponent.

B. Performance Metric

In this paper, we focus on the downlink performance of the SCS. In other words, we are concerned with the signal quality at a mobile-station (MS) within the SCS. The MS is assumed to be located at the origin of the l -D SCS unless specified otherwise. The signal quality at the MS is defined as the ratio of the received power from the serving BS to the sum of the interference powers (I or P_I), and the background noise power (η), and is called the signal-to-interference-plus-noise ratio (SINR). In an *interference-limited system*, $I \gg \eta$ and the signal quality is the signal-to-interference ratio (SIR).

Using (1), the SINR at the MS from a BS at a distance, say R_i , is

$$\text{SINR} = \frac{K_i \Psi_i / h(R_i)}{\sum_{\substack{j=1 \\ j \neq i}}^{\infty} K_j \Psi_j / h(R_j) + \eta}, \quad (2)$$

where $\{K_j, \Psi_j\}_{j=1}^{\infty}$ are independent and identically distributed (i.i.d) pairs of random variables representing the transmission power and the channel gain coefficients, respectively, of the j^{th} BS, and $\{R_j\}_{j=1}^{\infty}$ are random variables that come from underlying Poisson point process that governs the BS placement. Also, the MS associates itself with the BS that has the strongest received signal power (referred to as the serving BS), and can successfully communicate with this BS, only if the corresponding SINR exceeds a certain operating threshold, denoted by γ . In this paper, we find the tail probability [i.e. the complementary cumulative density function (c.c.d.f.)] of the SINR, which helps characterize an important performance metric for wireless networks, namely, the coverage probability, i.e. the probability that a MS is able to successfully communicate with the desired BS. The following section presents some necessary results that helps simplify and solve the problem.

III. SINR CHARACTERISTICS

As illustrated in Figure 1, this section presents several equivalence relations on BS density, path-loss model, transmission power and fading that leads to an equivalent canonical SCS model. Then the equivalence relations are used to simplify the analysis of the SINR. The equivalence is defined below.

Definition 2. Two SCSs are *equivalent* if the joint distribution of the powers from all the BSs of a SCS received at the MS located at the origin is the same as the joint distribution of the other SCS.

As a result, if the noise powers are equal, the SINRs at the MSs in two equivalent SCSs have the same distribution.

The following proposition gives an equivalent 1-D SCS for any l -D SCS. It is a simple consequence of the fact that the path-loss models considered in this paper is a function of only

the distance between the MS and a BS, not of the orientation.

Proposition 1. An l -D SCS, $l = 1, 2,$ and 3 is equivalent to a 1-D SCS with a one-sided BS density function $\lambda(r)$, $r \geq 0$, calculated below, if other parameters are the same.

- For a 1-D SCS with density function $d(x)$, $-\infty \leq x \leq \infty$, $\lambda(r) = d(r) + d(-r)$.
- For a 2-D SCS with density function $d(r, \theta)$, $\lambda(r) = \int_{\theta=0}^{2\pi} d(r, \theta) r d\theta$.
- For a 3-D SCS with density function $d(r, \theta, \phi)$, $\lambda(r) = \int_{\theta=0}^{\pi} \int_{\phi=0}^{2\pi} d(r, \theta, \phi) r^2 \sin(\theta) d\theta d\phi$.

Next, we show the equivalence between SCS's with path-loss model $\frac{1}{h(R)}$ and SCS's with path-loss model $\frac{1}{R}$, using the concepts of stochastic ordering [27]–[29].

Theorem 1. If other parameters are the same, a 1-D SCS with a BS density function $\lambda(r)$ and path-loss model $\frac{1}{h(R)}$ is equivalent to a 1-D SCS with a BS density function $\bar{\lambda}(r) = \lambda(h^{-1}(r)) \times \frac{d}{dr} h^{-1}(r)$, and path-loss model $\frac{1}{R}$, where R is the distance between a BS and the MS, as long as $h(r)$, $r \geq 0$ is a monotonically increasing function with a derivative $h'(r) > 0$, $\forall r > 0$ and an inverse $h^{-1}(r)$. As a result, if the noise powers are the same, the SINRs at the MSs located at the origin in the two SCSs have the same distribution, i.e. the SINR of (2) satisfies

$$\text{SINR}|_{\lambda(r)} \stackrel{=st}{=} \left. \frac{K_i \Psi_i / \tilde{R}_i}{\sum_{\substack{j=1 \\ j \neq i}}^{\infty} K_j \Psi_j / \tilde{R}_j + \eta} \right|_{\bar{\lambda}(r)}, \quad (3)$$

where $\left\{ \tilde{R}_j \right\}_{j=1}^{\infty}$ is the set of distances of BSs from the MS in the 1-D SCS with BS density function $\bar{\lambda}(r)$ and $\stackrel{=st}{=}$ represents the equivalence in distribution.

Proof: See Appendix A. ■

In the following theorem, we show the equivalence between SCS's with random transmission power and fading and SCS's with deterministic transmission power and fading.

Theorem 2. A 1-D SCS with BS density function $\lambda(r)$, path-loss model $\frac{1}{R}$, random transmission power K and random fading Ψ that are i.i.d. across all BSs, is equivalent to another 1-D SCS with a BS density function $\bar{\lambda}(r)$, $\frac{1}{R}$ path-loss model, unity transmission power and unity fading. The

above is true for arbitrary joint distributions of (K, Ψ) as long as $\bar{\lambda}(r) = \mathbb{E}_{K, \Psi} [K \Psi \lambda(K \Psi r)] < \infty$ holds for all $r \geq 0$, where $\mathbb{E}_{K, \Psi} [\cdot]$ is the expectation operator w.r.t. (K, Ψ) . The distributions of the SINRs at the MSs located at the origin of the two SCS's are the same if the noise powers of the MSs are equal.

Proof: See Appendix B. ■

Combining Proposition 1, Theorem 1 and Theorem 2, without loss of generality, we can now restrict our attention to the SINR characterization of the canonical SCS defined below.

Definition 3. A canonical SCS is a 1-D SCS with a BS density function $\lambda(r)$, $r \geq 0$, unity transmission power and unity fading factors for all BSs in the SCS, and a path-loss model of $\frac{1}{R}$.

For a canonical SCS, the BS closest to the origin is the serving BS and the rest of the BSs contribute to the interference power. The following is an interesting fact.

Lemma 1. If the noise powers are the same, the distributions of SINRs at the MS in canonical SCSs with BS density function of the form $\frac{1}{a}\lambda(\frac{r}{a})$ are the same for all $a > 0$. In other words, $\text{SINR}|_{\lambda(r)} =_{\text{st}} \text{SINR}|_{\frac{1}{a}\lambda(\frac{r}{a})}$.

Proof: See Appendix C. ■

As a result, the appropriate scaling of the BS density function will not change the p.d.f. of SINR. Next, we derive expressions for the tail probability of the SINR.

Theorem 3. The tail probability of SINR at the MS in a canonical SCS, $\mathbb{P}(\{\text{SINR}_{\text{canonical}} > \gamma\})$ is given by

$$\mathbb{P}(\{\text{SINR}_{\text{canonical}} > \gamma\}) = \begin{cases} \int_{\omega=-\infty}^{\infty} \Phi_{\frac{1}{\text{SINR}_{\text{canonical}}}}(\omega) \left(\frac{1 - \exp(-\frac{i\omega}{\gamma})}{i\omega} \right) \frac{d\omega}{2\pi}, & \gamma > 0 \\ 1, & \gamma = 0 \end{cases}, \quad (4)$$

where $\Phi_{\frac{1}{\text{SINR}_{\text{canonical}}}}(\omega)$ is the characteristic function of $\frac{1}{\text{SINR}_{\text{canonical}}}$ given by

$$\Phi_{\frac{1}{\text{SINR}_{\text{canonical}}}}(\omega) = \mathbb{E}_{R_1} \left[\exp(i\omega\eta R_1) \times \Phi_{P_I|R_1}(\omega R_1 | R_1) \right] \quad (5)$$

$$= \mathbb{E}_{R_1} \left[\exp(i\omega\eta R_1) \exp \left(R_1 \times \int_{u=1}^{\infty} \left(\exp\left(\frac{i\omega}{u}\right) - 1 \right) \lambda(uR_1) du \right) \right] \quad (6)$$

where $\mathbb{E}_{R_1}[\cdot]$ is the expectation w.r.t. the random variable R_1 , which is the distance of the BS closest to the origin, and with the probability density function (p.d.f.) $f_{R_1}(r) = \lambda(r) \times e^{-\int_{s=0}^r \lambda(s) ds}$, $r \geq 0$.

Proof: See Appendix D. ■

Now, we take a minor detour from studying the canonical SCS and consider a 1-D SCS affected by i.i.d. random fading factor with unity mean exponential distribution. For this case, the following theorem gives a simpler expression for the tail probability of SINR when $\gamma \geq 1$.

Theorem 4. For a 1-D SCS with a BS density function $\bar{\lambda}(r)$, $\frac{1}{R}$ path-loss model, unity transmission power, i.i.d. unity mean exponential random variable for fading at each BS, the tail probability of SINR for $\gamma \geq 1$ is given by

$$\mathbb{P}(\{\text{SINR} > \gamma\}) = \int_{r=0}^{\infty} \bar{\lambda}(r) \exp \left(-\eta\gamma r - \int_{s=0}^{\infty} \frac{\bar{\lambda}(s) ds}{1 + (\gamma r)^{-1} s} \right) dr. \quad (7)$$

Proof: See Appendix E. ■

The above result can be used for a canonical SCS under certain conditions. We briefly investigate this situation for which we define $\mathcal{L}(f(x), s) \triangleq \int_{x=0}^{\infty} e^{-sx} f(x) dx$ to be the unilateral Laplace transform of the function $f(x)$.

Lemma 2. A canonical SCS with BS density function $\lambda(r)$ is equivalent to the 1-D SCS considered in Theorem 4 if there exists a continuous BS density function $\bar{\lambda}(r) \geq 0$ such that

$$\mathcal{L} \left(\bar{\lambda}(x), \frac{1}{r} \right) = \int_{s=0}^r \lambda(s) ds, \quad \forall r \geq 0. \quad (8)$$

As a result, the tail probability of SINR for such canonical SCS is equal to (7).

Proof: The above result is obtained as a consequence of Theorem 2 which says that the

two SCSs considered above are equivalent if $\lambda(r) = \mathbb{E}_\Psi [\Psi \bar{\lambda}(r\Psi)]$, $\forall r \geq 0$, where Ψ is the unity mean exponential random variable representing the fading factors in the latter SCS. By rewriting the expectation in the above equation as an integral and simplifying, we obtain

$$\lambda(r) = \int_{x=0}^{\infty} \frac{d}{dr} \left(e^{-\frac{x}{r}} \right) \bar{\lambda}(x) dx \stackrel{(a)}{=} \frac{d}{dr} \left(\mathcal{L} \left(\bar{\lambda}(x), \frac{1}{r} \right) \right),$$

where (a) is obtained by exchanging the order of integration and differentiation, which is valid since $\bar{\lambda}(r)$ is continuous. Further, the resultant integral can be written in terms of the Laplace transform of $\bar{\lambda}(x)$. Using $\mathcal{L} \left(\bar{\lambda}(x), \frac{1}{r} \right) \Big|_{r=0} = 0$ as the initial condition, the above differential equation can be solved to obtain the condition for equivalence between the two SCSs to be (8). ■

The following shows examples for the existence of BS density functions $(\lambda(r), \bar{\lambda}(r))$ that satisfy the condition in (8).

Example 1. Polynomial - polynomial equivalence: The pair $(\lambda(r), \bar{\lambda}(r)) = (\alpha_1 r^\delta, \alpha_2 r^\delta)$ satisfy the condition in (8) as long as $\delta + 1 > 0$, and $\alpha_1 = \alpha_2 \Gamma(1 + \delta) > 0$, where $\Gamma(\cdot)$ is the Gamma function.

Example 2. Rational - exponential equivalence: The pair $(\lambda(r), \bar{\lambda}(r)) = \left(\frac{1}{(1+\alpha r)^2}, e^{-\alpha r} \right)$, $\forall \alpha > 0$ satisfy the condition in (8).

We will see in the following section that the equivalent 1-D BS density function for the homogeneous l -D SCSs are polynomial functions, and using Example 1 and Theorem 4, simple analytical expressions the tail probability of SINR are obtained.

The results presented in this section can together accurately characterize the SINR in any arbitrary SCS with arbitrary transmission and channel characteristics. The semi-analytical expressions presented above might seem unwieldy at the first glance. But it turns out that several insightful results can be extracted from this representation for a special class of SCSs that are practically important and popular in literature. This special class of SCSs are the homogeneous l -D SCSs, $l \in \{1, 2, 3\}$, and we dedicate the next section to studying this special class in detail.

IV. HOMOGENEOUS l -D SCS

In this section, we focus on the analysis of the homogeneous l -D SCSs with a power-law path-loss model $h(R) = R^\varepsilon$. The homogeneous l -D SCS is the most widely used stochastic geometric model in the literature for modeling arrangement of node locations. Especially, its validity in the study of the small-cell networks is extremely appealing. Moreover, this model has the advantage of being analytically amenable for a variety of situations that are of great importance in the modeling and analysis of any type of wireless network. The results provide several insights about such large-scale networks that can be applied in the design of actual networks in practice. Next, we apply the results of the previous section to the case of the homogeneous l -D SCS.

Corollary 1. [of Proposition 1] A homogeneous l -D SCS with a constant BS density λ_0 over the entire space is equivalent to the 1-D SCS with a BS density function $\lambda(r) = \lambda_0 b_l r^{l-1}$, $\forall r \geq 0$, where $b_1 = 2$, $b_2 = 2\pi$, $b_3 = 4\pi$.

This is easily proved by letting $d(x)$, $d(r, \theta)$, and $d(r, \theta, \phi)$ be λ_0 in Proposition 1.

For the power-law path-loss model $h(R) = R^\varepsilon$, we have the following equivalent SCS using Corollary 1 and Theorem 2.

Corollary 2. [of Theorem 2] A homogeneous l -D SCS with BS density λ_0 and path-loss model $\frac{1}{R^\varepsilon}$ is equivalent to the 1-D SCS with a BS density function $\bar{\lambda}(r) = \lambda_0 \frac{b_l}{\varepsilon} r^{\frac{l}{\varepsilon}-1}$, $r \geq 0$ and the path-loss model $\frac{1}{R}$.

Next, we characterize the effect of random transmission powers and fading factors, i.i.d. across BSs in the homogeneous l -D SCS.

Corollary 3. [of Theorem 2] A homogeneous l -D SCS with BS density λ_0 , power-law path-loss model $(\frac{1}{R^\varepsilon})$, random transmission powers and fading factors that have arbitrary joint distribution and are i.i.d. across all the BSs is equivalent to another homogeneous l -D SCS with a BS density $\bar{\lambda} = \lambda_0 \mathbb{E} \left[(K\Psi)^{\frac{l}{\varepsilon}} \right]$, same power-law path-loss model $(\frac{1}{R^\varepsilon})$, unity transmission power and unity fading factor at each BS, where K , Ψ have the same joint distribution as the transmission power and fading factors of the original homogeneous l -D SCS and $\mathbb{E}[\cdot]$ is the expectation operator

w.r.t. K and Ψ , as long as $\mathbb{E} \left[(K\Psi)^{\frac{l}{\varepsilon}} \right] < \infty$.

Proof: Using Corollary 1 and Corollary 2, we obtain a 1-D SCS with BS density function $\tilde{\lambda}(r) = \lambda_0 \frac{b_l}{\varepsilon} r^{\frac{l}{\varepsilon}-1}$, with a path-loss model $\frac{1}{R}$. Now, from Theorem 2, the equivalent canonical SCS has a BS density function $\hat{\lambda}(r) = \mathbb{E} \left[(K\Psi)^{\frac{l}{\varepsilon}} \right] \times \tilde{\lambda}(r)$. As a result, this can be traced back to the scaling of the BS density of the original homogeneous l -D SCS by $\mathbb{E} \left[(K\Psi)^{\frac{l}{\varepsilon}} \right]$. ■

As a result, we can restrict our attention to SINR characterization when all the BSs of the l -D SCS have unity transmission power and fading factors. Now, we give the expression for the tail probability of SINR in a homogeneous l -D SCS.

Corollary 4. [of Theorem 3] In a homogeneous l -D SCS with a BS density λ_0 , unity transmission power and fading factor at each BS, if the path-loss exponent of the power-law path-loss model satisfies $\varepsilon > l$, the characteristic function of the reciprocal of SINR is given by

$$\Phi_{\frac{1}{\text{SINR}}}(\omega) = \mathbb{E}_{R_1} \left[e^{i\omega\eta R_1} \times e^{\frac{\lambda_0 b_l}{l} R_1^{\frac{l}{\varepsilon}} ({}_1F_1(-\frac{l}{\varepsilon}; 1-\frac{l}{\varepsilon}; i\omega))} \right], \quad (9)$$

where the p.d.f. of R_1 is $f_{R_1}(r) = \lambda_0 \frac{b_l}{\varepsilon} r^{\frac{l}{\varepsilon}-1} \cdot e^{-\lambda_0 \frac{b_l}{l} r^{\frac{l}{\varepsilon}}}$, $r \geq 0$. When $\eta = 0$, the SINR is equivalently the signal-to-interference ratio (SIR), and

$$\Phi_{\frac{1}{\text{SIR}}}(\omega) = \frac{1}{{}_1F_1\left(-\frac{l}{\varepsilon}; 1-\frac{l}{\varepsilon}; i\omega\right)}, \quad (10)$$

where ${}_1F_1(\dots)$ is the confluent hypergeometric function of the first kind [30]. The tail probability of SINR is given by (4).

Proof: From Corollary 2, the SINR distribution is equivalent to the canonical SCS with BS density function $\lambda(r) = \lambda_0 \frac{b_l}{\varepsilon} r^{\frac{l}{\varepsilon}-1}$, $r \geq 0$. Now, by solving for (6), in Theorem 3, we obtain (9). Further, the expectation in (9) reduces to (10). ■

Due to Corollary 3, the homogeneous l -D SCS satisfies the conditions in Theorem 4 and hence a simple expression for the tail probability of SINR for $\gamma \geq 1$ can be derived below.

Corollary 5. [of Theorem 4] For a homogeneous l -D SCS with BS density λ_0 , path-loss model $\frac{1}{R^\varepsilon}$, $\varepsilon > l$, with unity transmission power and fading factor at each BS, the tail probability of

SINR for $\gamma \geq 1$ is

$$\mathbb{P}(\{\text{SINR} > \gamma\}) = \int_{r=0}^{\infty} \frac{\lambda_0 b_l r^{l-1}}{\Gamma(1 + \frac{l}{\varepsilon})} \exp\left(-\eta \gamma r^\varepsilon - \frac{\lambda_0 b_l r^l \pi \gamma^{\frac{l}{\varepsilon}}}{\varepsilon \Gamma(1 + \frac{l}{\varepsilon}) \sin(\frac{l\pi}{\varepsilon})}\right) dr, \quad (11)$$

and when $\eta = 0$, the tail probability of SIR is

$$\mathbb{P}(\{\text{SIR} > \gamma\}) = \frac{\sin(\frac{l\pi}{\varepsilon}) \gamma^{-\frac{l}{\varepsilon}}}{(\frac{l\pi}{\varepsilon})} = \text{sinc}\left(\frac{l}{\varepsilon}\right) \gamma^{-\frac{l}{\varepsilon}}. \quad (12)$$

Proof: Due to Corollary 3, the homogeneous l -D SCS is equivalent to another homogeneous l -D SCS with the same path-loss model and transmission powers as the former, and with a BS density $\frac{\lambda_0}{\Gamma(1 + \frac{l}{\varepsilon})}$ and i.i.d. unity mean exponential random fading factors at each BS. Using Corollary 2, the BS density function of the 1-D SCS with $\frac{1}{R}$ path-loss model that is equivalent to the latter homogeneous l -D SCS is $\bar{\lambda}(r) = \frac{\lambda_0 b_l r^{\frac{l}{\varepsilon}-1}}{\varepsilon \Gamma(1 + \frac{l}{\varepsilon})}$, $r \geq 0$. An alternate approach to obtain the expression for $\bar{\lambda}(r)$ is using Lemma 2 and Example 1.

For the 1-D SCS, Theorem 4 is used to obtain the expression for the tail probability of SINR to be (11), using the identity $\int_{s=0}^{\infty} \frac{s^{\frac{l}{\varepsilon}-1} ds}{1 + (\gamma r) s} = \frac{\pi(\gamma r)^{\frac{l}{\varepsilon}}}{\sin(\frac{l\pi}{\varepsilon})}$. Finally, (12) is obtained by substituting $\eta = 0$ in (11) and evaluating the outer integral. This completes the proof. \blacksquare

Using Corollaries 4 and 5, the expression for the tail probability of SINR in a homogeneous l -D SCS with random transmission power and fading factor with an arbitrary joint distribution that are i.i.d. across the BSs of the SCS can be obtained by merely scaling the BS density λ_0 with an appropriate constant that is given in Corollary 3.

The following lemma shows another interesting property of the SINR distribution in a homogeneous l -D SCS.

Lemma 3. The SINR distribution in a homogeneous l -D SCS with a constant BS density λ_0 , path-loss model $\frac{1}{R^\varepsilon}$, unity transmission power and fading factor at each BS with a background noise power η is the same as in a homogeneous l -D SCS with the same path-loss model, unity BS density, unity transmission power and fading factor at each BS and a background noise power

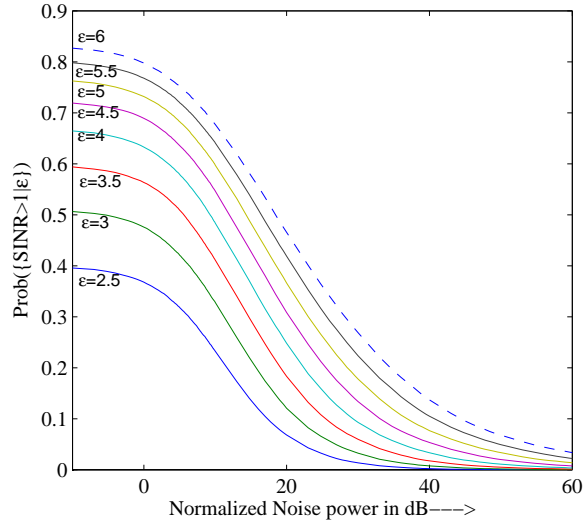


Figure 3: Plot of $\text{Prob}(\{\text{SINR} > 1\})$ vs Noise power

$\eta\lambda_0^{-\frac{\epsilon}{l}}$. Equivalently,

$$\text{SINR}|_{(\lambda_0, \epsilon, \eta)} \stackrel{=st}{=} \text{SINR}|_{\left(1, \epsilon, \eta\lambda_0^{-\frac{\epsilon}{l}}\right)}. \quad (13)$$

$$\text{Proof: } \text{SINR}|_{(\lambda_0, \epsilon, \eta)} \stackrel{(a)}{=} \frac{R_1^{-\epsilon}}{\sum_{k=2}^{\infty} R_k^{-\epsilon} + \eta} \Big|_{\lambda_l(r)} \stackrel{(b)}{=} \frac{(\alpha R_1)^{-\epsilon}}{\sum_{i=2}^{\infty} (\alpha R_i)^{-\epsilon} + \eta\alpha^{-\epsilon}} \Big|_{\lambda_l(r)} \stackrel{(b)}{=} \frac{(R'_1)^{-\epsilon}}{\sum_{k=2}^{\infty} (R'_k)^{-\epsilon} + \bar{\eta}} \Big|_{\frac{1}{\alpha}\lambda_l\left(\frac{r}{\alpha}\right)},$$

where $\alpha = \lambda_0^{\frac{1}{l}}$; $\bar{\eta} = \eta\alpha^{-\epsilon}$; (a) is obtained by expressing SINR in terms of the equivalent 1-D SCS with $\lambda_l(r) = \lambda_0 b_l r^{l-1}$, $r \geq 0$, and multiplying numerator and denominator with $\alpha^{-\epsilon}$; (b) follows from Corollary 1; and finally, (13) is obtained by noting that the 1-D SCS with BS density function $\frac{1}{\alpha}\lambda_l\left(\frac{r}{\alpha}\right)$ in (b) corresponds to a homogeneous l -D SCS with BS density 1. ■

Therefore, it is sufficient to analyze a homogeneous l -D SCS with BS density $\lambda_0 = 1$ and maintain a lookup table for the tail probability of SINR for different values of the noise powers and path-loss exponents using (4). The lookup table is presented for a homogeneous 2-D SCS in Figure 3 as a plot of $\mathbb{P}(\{\text{SINR} > 1\})$ against noise powers for different values of path-loss exponents. Further, in a homogeneous l -D SCS with a high BS density λ_0 , the equivalent noise power $\eta\lambda_0^{-\frac{\epsilon}{l}}$ is small according to Lemma 3. Hence, in an *interference-limited system* (large λ_0), the signal quality can be measured in terms of SIR. Further remarks on SIR of a homogeneous

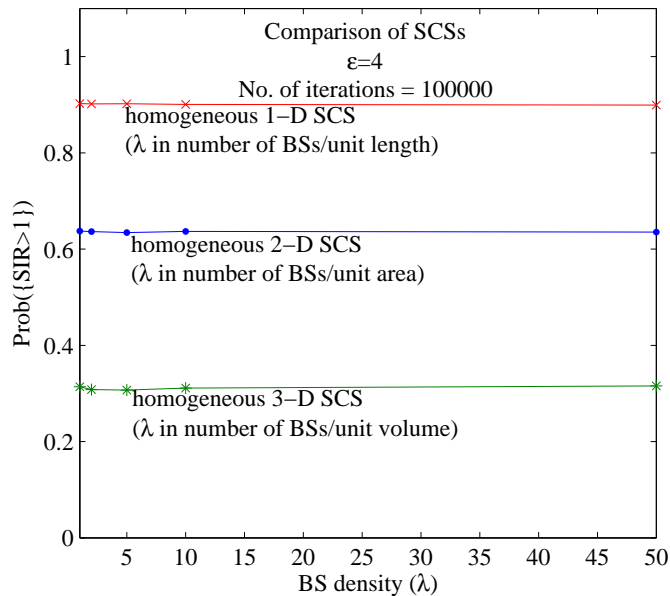


Figure 4: Simulation showing the invariance of the performance of homogeneous l -D SCS on the BS density.

l -D SCS based on Corollaries 4 are given below.

Remark 1. The characteristic function of the $\frac{1}{\text{SIR}}$ does not depend on λ_0 , and hence the tail probability of SIR at a MS in a homogeneous l -D SCS does not depend on λ_0 .

Remark 2. From Corollary 1 and Remark 1, the tail probability of SIR is invariant to random transmission powers and fading factors with arbitrary joint distribution and i.i.d. across the BSs.

Remark 3. The expression for the characteristic function of $\frac{1}{\text{SIR}}$ for a *homogeneous* 2-D and 3-D SCS is same as that of a *homogeneous* 1-D SCS with path-loss exponents $\frac{\epsilon}{2}$ and $\frac{\epsilon}{3}$, respectively.

Remark 1 shows why the tail probabilities of SIR as a function of BS density for the *homogeneous* 1-D, 2-D and 3-D SCSs in Figure 4 are constant¹. Remark 3 helps build an intuition of why the *homogeneous* 1-D SCS has a higher tail probability of SIR than *homogeneous* 2-D and 3-D SCSs. As the path-loss exponent decreases, the BSs farther away from the MS have a greater contribution to the total interference power at the MS, and this leads to a poorer SIR at the

¹The simulation results in this section are based on the methods in Appendix H.

MS and a smaller tail probability. Figure 4 shows the tail probabilities of SIR in a *homogeneous* 1-D SCS as a function of the path-loss exponent ε ; the squares (\square) and the pluses ($+$) represent the values computed analytically and by Monte-Carlo simulations, respectively. According to Remark 3, the same figure can be used for 2-D and 3-D systems using the scaling of $\frac{\varepsilon}{2}$, and $\frac{\varepsilon}{3}$ respectively.

In the following, we present an approximation to SIR based on modeling the interference due to the strongest few BSs accurately and the interference due to the rest by their ensemble average. The approximation is expected to be tight for low BS densities. Due to Remark 1, the same approximation will be tight for all BS densities. Now, we define the so-called *few BS approximation* and derive closed form expressions for the tail probability of SIR at MS in a *homogeneous* l -D SCS for both the SIR regions $[0, 1)$ and $[1, \infty)$.

Definition 4. *The few BS approximation* corresponds to modeling the total interference power at the MS in a SCS as the sum of the contributions from the strongest few interfering BSs and an ensemble average of the contributions of the rest of the interfering BSs.

Recall that the total interference power is $P_I = \sum_{i=2}^{\infty} R_i^{-\varepsilon}$, where $\{R_i\}_{i=1}^{\infty}$ is the set of distances of BSs arranged in the ascending order of their separation from the MS. The arrangement also corresponds to the descending order of their contribution to P_I , due to path-loss. In the few BS approximation, P_I is approximated by $\tilde{P}_I(k) = \sum_{i=2}^k R_i^{-\varepsilon} + \mathbb{E}[\sum_{i=k+1}^{\infty} R_i^{-\varepsilon} | R_k]$, for some k , where $\mathbb{E}[\cdot]$ is the expectation operator and corresponds to the ensemble average of the contributions of BSs beyond R_k . The SIR at the MS obtained by the few BS approximation is denoted by SIR_k . The expectation is calculated as follows.

Lemma 4. For a homogeneous l -D SCS, with BS density λ_0 and $\varepsilon > l$, for $k = 1, 2, 3, \dots$,

$$\mathbb{E} \left[\sum_{i=k+1}^{\infty} R_i^{-\varepsilon} \middle| R_k \right] = \frac{\lambda_0 b_l R_k^{l-\varepsilon}}{\varepsilon - l}. \quad (14)$$

Proof: Firstly, use Corollary 1 to reduce the l -D SCS to an equivalent 1-D SCS with BS density function $\lambda(r) = \lambda_0 b_l r^{l-1}$, $\forall r \geq 0$. Next, given k , using the Superposition theorem of Poisson processes, the original Poisson process is equivalent to the union of two independent

Poisson processes defined in the non-overlapping regions $[0, R_k]$ and (R_k, ∞) , respectively, with the same BS density function. Now, using Campbell's theorem [26, Page 28] to the Poisson process defined in (R_k, ∞) , we obtain (14). ■

The following theorem gives the SIR tail probability approximation, using $k = 2$.

Theorem 5. In a homogeneous l -D SCS with BS density λ_0 and path-loss exponent ε , satisfying $\varepsilon > l$, the tail probability of SIR_2 at the MS is given by

$$\mathbb{P}(\{\text{SIR}_2 > \gamma\}) = \begin{cases} \gamma^{-\frac{l}{\varepsilon}} C_{\frac{\varepsilon}{l}}, & \gamma \geq 1 \\ 1 - e^{-u(\gamma)}(1 + u(\gamma)) + \gamma^{-\frac{l}{\varepsilon}} D_{\frac{\varepsilon}{l}}(\gamma), & \gamma \leq 1 \end{cases}, \quad (15)$$

where $C_{\frac{\varepsilon}{l}} = G(0)$ and $D_{\frac{\varepsilon}{l}}(\gamma) = G(u(\gamma))$ with $G(a) = \int_{v=a}^{\infty} \frac{ve^{-v}}{(1+v(\frac{\varepsilon}{l}-1))^{-1})^{\frac{l}{\varepsilon}}} dv$, and $u(\gamma) \equiv (\frac{\varepsilon}{l} - 1) \left(\frac{1}{\gamma} - 1\right)$.

Proof: See Appendix F. ■

The above approximation can be further tightened by recalling that we already have a simple closed-form expression in (12) for the tail probability of SIR for values in the range $[1, \infty)$. Hence, the new approximation is as follows

$$\mathbb{P}(\{\text{SIR}_{approx} > \gamma\}) = \begin{cases} \mathbb{P}(\{\text{SIR} > \gamma\}) & , \gamma \geq 1 \\ \mathbb{P}(\{\text{SIR}_2 > \gamma\}) & , \gamma \leq 1 \end{cases}, \quad (16)$$

where the relevant quantities are obtained from (12) and Theorem 5.

Notice that $\mathbb{P}(\{\text{SIR} > \gamma\}) = \frac{\text{sinc}(\frac{l}{\varepsilon})}{C_{\frac{\varepsilon}{l}}} \mathbb{P}(\{\text{SIR}_2 > \gamma\})$ for $\gamma \geq 1$. Figure 5a shows that the few BS approximation (●) closely follows the actual behavior (□). Figure 5b shows the comparison of the tail probabilities of SIR (computed using Corollaries 4 and 5) and SIR_2 for a *homogeneous* 2-D SCS with path-loss exponent 4. Notice that the gap between the two tail probability curves is negligible in the region $\gamma \in [0, 1]$, and further, both the curves are straight lines parallel to each other in the region $\gamma \in [1, \infty)$, when the tail probability is plotted against γ , both in the logarithmic scale. This shows that the few BS approximation characterizes the signal quality in closed form and is a good approximation for the actual SIR.

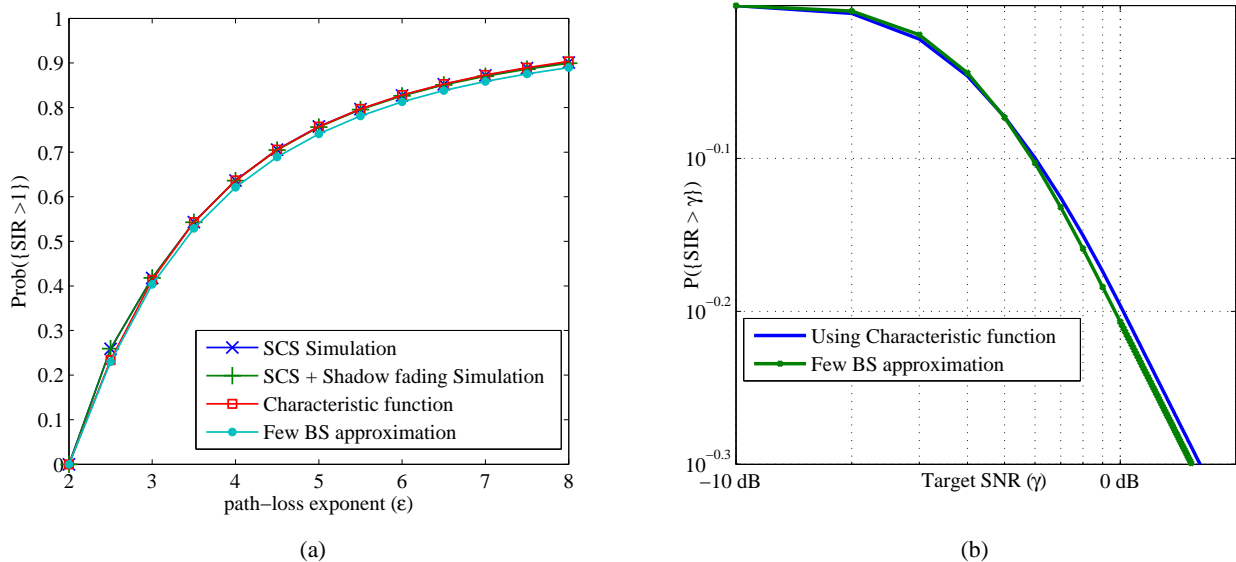


Figure 5: (a) Comparison of Simulations with the analytical results, (b) Homogeneous 2-D SCS: Comparing exact SIR and the few BS approximation for path-loss $\varepsilon = 4$.

Now, having characterized the SIR for the homogeneous l -D SCS, we look closely into what happens when $\varepsilon \leq l$. We will restrict ourselves to the case when $l = 2$, and the steps are similar for $l = 1$, and $l = 3$.

Theorem 6. A homogeneous 2-D SCS with BS density λ , where the signal decays according to a power-law path-loss function with a path-loss exponent $\varepsilon \leq 2$, the SIR at the MS is 0 with probability 1.

Proof: See Appendix G for the case $\varepsilon = 2$. From [15, Corollary 5], $\mathbb{P}(\{\text{SIR} > \gamma\})|_{\varepsilon < 2} \leq \mathbb{P}(\{\text{SIR} > \gamma\})|_{\varepsilon = 2} = 0$, $\forall \gamma \geq 0$. Hence we have proved the above result. ■

Note that once we have characterized the SINR distribution, the outage probability at the MS is known. The event that the MS is in coverage is given by $\{\text{SINR} > \gamma\}$, where γ is the SINR threshold that the MS should satisfy to be in coverage. Consequently, the coverage probability, $\mathbb{P}(\{\text{SINR} > \gamma\})$ is precisely the tail probability of SINR computed at γ . Next, we study the average ergodic reception rate for an MS in coverage. This quantity, termed as the coverage conditional average rate, is given by $\mathcal{R} = \mathbb{E}[\log(1 + \text{SINR}) | \{\text{SINR} > \gamma\}]$ and is the average

of the instantaneous rate achievable at the MS when the interference is considered as noise. The coverage conditional average rate at the MS simplifies to the following expression.

$$\mathcal{R} = \log(1 + \gamma) + \int_{t=\Gamma}^{\infty} \frac{\mathbb{P}(\{\text{SINR} > t\})}{(1+t)\mathbb{P}(\{\text{SINR} > \gamma\})} dt.$$

As a result, based on Proposition 1 and Theorems 1 - 4, we can compute the coverage conditional average rate for any SCS. Specifically, in the interference-limited case, the following proposition provides the expression for a homogeneous l -D SCS and when the popular power-law path-loss model is assumed. For this case, the SIR characteristics are invariant to the randomness in the transmission powers and the fading factors due to Remark 2. Hence, without loss of generality, we restrict our attention to the case of constant transmission powers at all BSs and no fading.

Proposition 2. The ergodic average rate at the MS in a homogeneous 2-D SCS under the power-law path-loss model, with constant transmission powers at all BSs and no fading is given by

$$\mathcal{R} = \log(1 + \gamma) + \int_{x=\gamma}^{\alpha} \frac{\mathbb{P}(\{\text{SIR} > x\})}{\mathbb{P}(\{\text{SIR} > \gamma\})(1+x)} dx + \alpha^{-\frac{2}{\varepsilon}} \frac{\varepsilon}{2} \cdot {}_2F_1\left(1, \frac{2}{\varepsilon}; 1 + \frac{2}{\varepsilon}; -\alpha^{-1}\right),$$

where $\alpha = \max(\gamma, 1)$, where ${}_2F_1\left(1, \frac{2}{\varepsilon}; 1 + \frac{2}{\varepsilon}; -\alpha^{-1}\right)$ is the Gauss hypergeometric function and the probabilities are computed using (4). Note that for $\gamma \geq 1$, the middle term drops out.

V. NUMERICAL EXAMPLE AND DISCUSSION

In the first example, we consider a homogeneous 2-D SCS with $\lambda = 0.01$, a power-law path-loss model with path-loss exponent 4, and a background noise power of -10 dB and unity transmission powers. We compare the SINR tail probabilities for several cases where we vary the distributions of the fading factors as well as the background noise power. Notice in Figure 6a that in the case when there is background noise, the distribution of the fading greatly affects the SINR performance at the MS. In the presence of the background noise, the MS sees a better SINR performance when the fading factors are i.i.d. exponential random variables than when the fading factors are log-normal random variables, when they have the same mean, and the SINR

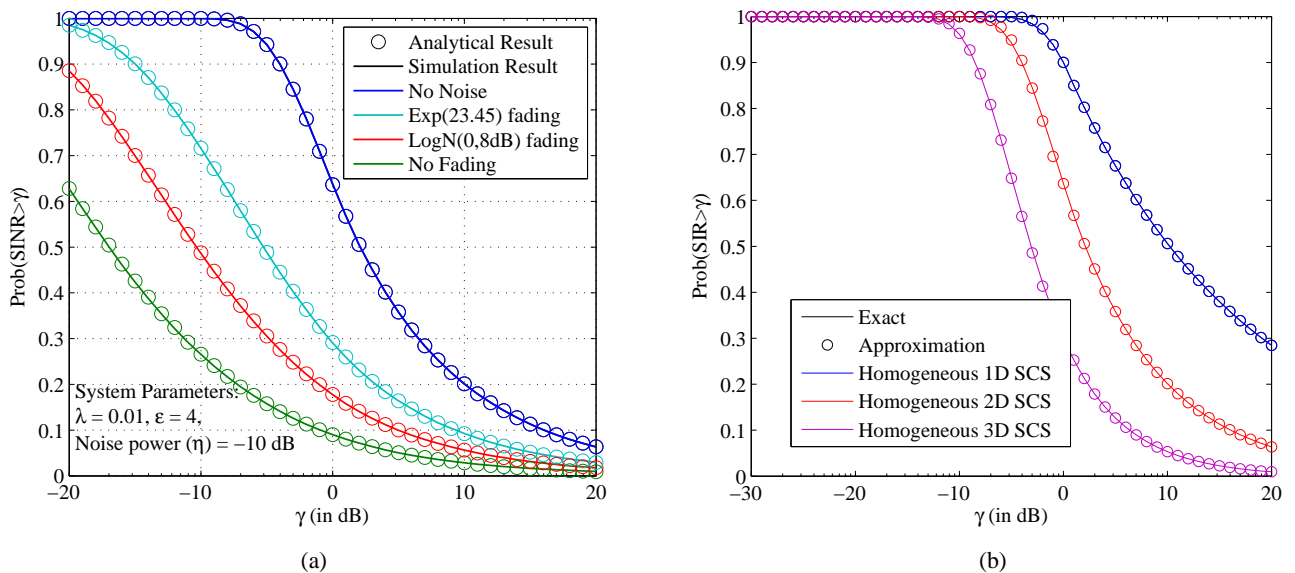


Figure 6: (a) Comparing the SINR distributions for various fading distributions and noise profiles, (b) Evaluating the tightness of the few-BS approximation

performance is far more superior than that without fading. This is justified by Corollary 3 and Corollary 3 where the equivalent homogeneous 2-D SCS with unity BS density has an equivalent background noise power for the log-normal fading case that is strictly greater than that for the exponential fading distributions. Further, in the no noise case, the SINR performance is invariant to the fading distribution and is the same as in the no fading case. This is also depicted in Figure 6a.

In Figure 6b, we assess the few-BS approximation for the SIR characterization in the homogeneous l -D SCS. This figure shows that the SIR approximation derived in Section IV based on the few-BS approximation (Equation (16)) closely follows the exact SIR characterization. Moreover, this relationship holds for a wide range of scenarios of interest such as for arbitrary fading and transmission power distributions, and for all BS densities. In the following section, we discuss the usage of the results obtained thus far in the analysis of other useful wireless communication scenarios.

VI. APPLICATIONS IN WIRELESS COMMUNICATIONS

We discuss several scenarios where the wireless communication systems are modeled by the *homogeneous* l -D SCS with BS density λ_0 , where $l = 1, 2$, and 3 correspond to highway, suburban, and dense urban deployments, respectively.

BSs with sectorized antennas: In this example, we give a practical scenario where the transmission powers of the BSs are i.i.d. random variables. For example, consider the case where each BS has an ideal sectorized antenna with gain G and beam-width θ , such that BS's antenna faces the MS with probability $\frac{\theta}{2\pi}$, in which case $K_i = G$, and otherwise $K_i = 0$. In this case, in the absence of fading, from Corollary 3, $\bar{\lambda}_0 = \lambda_0 G^{\frac{2}{\varepsilon}} \frac{\theta}{2\pi}$ is the BS density of the equivalent *homogeneous* l -D SCS.

Multiple Access Techniques: Next, we study the signal quality at the MS in a cellular system employing different multiple access techniques. For example, in a code division multiple access (CDMA) system, the goal is to maintain a constant voice signal quality at the MS, which is done by power control. This goal is achievable by having the serving BS increase its transmission power by $\alpha = \gamma \text{SIR}^{-1}$, where α is the power control factor or the processing gain, SIR is the instantaneous signal quality at the MS, and γ is the desired constant signal quality. In this formulation, α for each BS is a random variable and in general, the α 's of nearby BSs are correlated. But if the correlation is small, the SIR distribution computed here enables radio designers to approximately model the power needs to communicate with a MS in a SCS. In another formulation, if α is a constant factor by which the power of the serving BS is improved, its effect on the tail probability SIR at the MS is obtained by straightforward manipulations as $\mathbb{P}(\{\alpha \times \text{SIR} > \gamma | \varepsilon, l\}) = \text{sinc}\left(\frac{l}{\varepsilon}\right) \left(\frac{\gamma}{\alpha}\right)^{-\frac{l}{\varepsilon}}$ if $\gamma > \alpha$.

Then, consider frequency division multiple access (FDMA) and time division multiple access (TDMA) based cellular systems. Let the available spectrum (in frequency for FDMA and in time-slots for TDMA) be divided into N channel reuse groups (CG), and indexed as $k = 1, 2, \dots, N$. Then, each BS is assigned one of the N CGs, such that the k^{th} CG is assigned with probability p_k . In such a system, the MS chooses a CG that corresponds to the best SIR; the BS in the CG that corresponds to the strongest received power is the *desired* BS, and the MS chooses it as the

serving BS. The SIR at the MS in such a SCS is of interest to us. Note that this *homogeneous* l -D SCS is equivalent to N independent *homogeneous* l -D SCSs with constant BS densities $\lambda_0 p_1, \dots, \lambda_0 p_N$, by the properties of Poisson point processes. The tail probability of SIR at the MS in such a system is given by $\mathbb{P}(\{\text{SIR} > \gamma | \varepsilon, N\}) = 1 - [1 - \mathbb{P}(\{\text{SIR} > \gamma | \varepsilon\})]^N$, where the tail probability on the right hand side is computed using Corollary 4.

Cognitive Radios: In cognitive radio technology, the cognitive radio devices (or *secondary users*) opportunistically operate in licensed frequency bands occupied by *primary users*. The interference caused by *secondary user* transmissions is harmful for *primary users* operation, and is not acceptable beyond certain limits. Studying the nature of these interferences and formulating methods for addressing them has been an active area of research. The results in this paper are a rich source of mathematical tools for such studies. In [16], we have extensively applied the results developed here to understand the role of cooperation between the *secondary users* in ensuring that the interference caused by the *secondary users* are within the acceptable limits. The *secondary users* are modeled analogous to BS placement in *homogeneous* 1-D and 2-D SCS, and the tail probability of $\frac{C}{T}$ at the *primary user* is characterized. Further, in the context of radio environment map (REM, [16, and references therein]), we have highlighted the practical significance of the study of 1-D SCS.

Overlay Networks: The modern cellular communication network is a complex overlay of heterogeneous networks, such as macrocells, microcells, picocells and femtocells. This complex overlay network is seldom studied as is, due to the analytical intractabilities. In [2], [31], cellular systems consisting of macrocell and femtocell networks are analyzed. Using the results in our paper, the cumulative effect of all the networks constituting the overlay network, on the signal quality at the MS can be studied. A detailed study on this is set aside as a future work, while the preliminary results are presented in [17], [18]. Other efforts on the downlink performance characterization for heterogeneous networks can be found in [32], [32]–[37].

VII. CONCLUSIONS

In this paper, we study the characterization of the SIR and SINR at the MS in shotgun cellular systems where a SCS is defined as a cellular system where the BS deployment in a given region

is according to a Poisson point process. A sequence of equivalent SCSs are derived to show that it is sufficient to study the canonical SCS that has unity transmission power and unity fading factors, and a path-loss model of $\frac{1}{R}$. Analytical expressions for the tail probabilities of the SIR and SINR at the MS are obtained for 1-D, 2-D and 3-D SCSs, where the 1-D, 2-D and 3-D SCS are mathematical models for BS deployments along the highway (1-D), in planar regions (2-D) and in urban areas (3-D), respectively. Further, a closed form expression for the tail probability of SIR is derived for the homogeneous cases of 1-D, 2-D and 3-D SCS. The results are applicable for general fading distributions and arbitrary path-loss models. This makes the results useful for analyzing many different wireless scenarios that are characterized by uncoordinated deployments. The application of the results has been demonstrated in the study of the impact of cooperation between cognitive radios in the low power primary user detection and can be found in [16], and in the study of heterogeneous networks in [17]. Future work will further explore the applications of the SCS model in the context of indoor femtocells, cognitive radios, and multi-tier or overlay networks.

APPENDIX

A. Proof for Path-loss Equivalence Theorem (Theorem 1)

Let $\bar{R} = h(R)$ be the equivalent BS location. Using the *Mapping Theorem* in [26], BS with locations \bar{R} is also a Poisson point process, whose density is obtained below. For any non-homogeneous 1-D Poisson point process, $\mathbb{E}[N(r+s) - N(r)] = \int_r^{r+s} \lambda(z) dz$ is the expected number of occurrences in the interval $(r, r+s)$. Thus,

$$\begin{aligned} \mathbb{E}[N(r+s) - N(r)] &= \mathbb{E}[\text{Number of BSs with } \bar{R} \in (r, r+s)] \\ &= \mathbb{E}[\text{Number of BSs with } R \in (h^{-1}(r), h^{-1}(r+s))] \\ &= \int_{z=h^{-1}(r)}^{h^{-1}(r+s)} \lambda(z) dz = \int_{z=r}^{r+s} \frac{\lambda(h^{-1}(z))}{h'(h^{-1}(z))} dz. \end{aligned} \tag{17}$$

Hence, the 1-D SCS with path-loss model $\frac{1}{h(R)}$ and a BS density function $\lambda(r)$ is equivalent to the 1-D SCS with path-loss model $\frac{1}{R}$ and BS density function $\bar{\lambda}(r)$.

B. Proof for Arbitrary Fading Equivalence Theorem (Theorem 2)

Let $\bar{R} = R(K\Psi)^{-1}$, where R is the random variable representing the distance from the MS to a BS in the 1-D SCS with a BS density function $\lambda(r)$, K , Ψ are the transmission power and the fading factor corresponding to the BS, respectively, and \bar{R} is the corresponding equivalent distance. Using the *product space representation* and *Marking Theorem* in [26], \bar{R} also corresponds to the 1-D SCS with a BS density function derived following (17) :

$$\mathbb{E}[N(r+s) - N(r)] \stackrel{(a)}{=} \mathbb{E}_{K,\Psi} \left[\int_{rK\Psi}^{(r+s)K\Psi} \lambda(z) dz \right] \stackrel{(b)}{=} \int_r^{(r+s)} \mathbb{E}_{K,\Psi} [K\Psi\lambda(K\Psi z)] dz,$$

where (a) is obtained by rewriting the expectation with respect to each realization of Ψ and K , and (b) is obtained by exchanging the order of integration and expectation in (b) as $\mathbb{E}_{K,\Psi} [K\Psi\lambda(K\Psi z)] < \infty$. Hence, $\bar{R}'s$ corresponds to the 1-D SCS with a BS density function $\bar{\lambda}(r) = \mathbb{E}_{K,\Psi} [K\Psi\lambda(K\Psi r)]$.

C. Proof for Corollary 1

Let $\{R_k\}_{k=1}^{\infty}$ correspond to the 1-D SCS with BS density function $\lambda(r)$. Then, since the ordered base station locations R_k 's are determined by inter-base station distances, it follows that $\text{SINR}|_{\lambda(r)} \stackrel{(a)}{=} \frac{(aR_1)^{-1}}{\sum_{k=2}^{\infty} (aR_k)^{-1} + \eta} \Big|_{\lambda(r)} \stackrel{(b)}{\text{st}} \frac{(R'_1)^{-1}}{\sum_{k=2}^{\infty} (R'_k)^{-1} + \eta} \Big|_{\frac{1}{a}\lambda(\frac{r}{a})}$, where the SINR expression is obtained using (2) with $h(R) = R$, (a) is obtained by multiplying the numerator and denominator by $\frac{1}{a}$, $a > 0$ (b) follows from the properties of Poisson point processes. Further, $\{R'_k\}_{k=1}^{\infty}$ in (b) correspond to 1-D SCS with BS density $\frac{1}{a}\lambda(\frac{r}{a})$, $a > 0$.

D. Proof for the Tail Probability of SINR (Theorem 3)

The following are the sequence of step to derive the expression in (4).

$$\begin{aligned} \mathbb{P}(\{\text{SINR}_{\text{canonical}} > \gamma\}) &= \mathbb{P}\left(\left\{\frac{1}{\text{SINR}_{\text{canonical}}} < \frac{1}{\gamma}\right\}\right) \\ &\stackrel{(a)}{=} \int_{x=0}^{\frac{1}{\gamma}} \int_{\omega=-\infty}^{\infty} \Phi_{\frac{1}{\text{SINR}_{\text{canonical}}}}(\omega) e^{-i\omega x} \frac{d\omega}{2\pi} dx, \end{aligned}$$

where (a) is obtained by rewriting the c.d.f. of $\frac{1}{\text{SINR}_{\text{canonical}}}$ in terms of the characteristic function of $\frac{1}{\text{SINR}_{\text{canonical}}}$, where the inner integration computes the p.d.f. of $\frac{1}{\text{SINR}_{\text{canonical}}}$, and the outer

integration gives the c.d.f. at $\frac{1}{\gamma}$. When $\gamma = 0$, the above event occurs with probability 1, and otherwise, it is expressed in terms of the integration in (4) which is obtained by exchanging the order of integrations in (a), which is valid in this case, and then evaluating the integral w.r.t. x . In the rest of this section, we derive the expression for $\Phi_{\frac{1}{\text{SINR}_{\text{canonical}}}}(\omega)$, by first noting that

$$\text{SINR}_{\text{canonical}} = \frac{R_1^{-1}}{\sum_{k=2}^{\infty} R_k^{-1} + \eta}.$$

$$\begin{aligned} \Phi_{\frac{1}{\text{SINR}_{\text{canonical}}}}(\omega) &\stackrel{(a)}{=} \mathbb{E}_{R_1} \left[\Phi_{\frac{1}{\text{SINR}_{\text{canonical}}}} \Big|_{R_1}(\omega | R_1) \right] \stackrel{(b)}{=} \mathbb{E}_{R_1} \left[e^{i\omega\eta R_1} \Phi_{\frac{\sum_{k=2}^{\infty} R_k^{-1}}{R_1^{-1}}} \Big|_{R_1}(\omega | R_1) \right] \\ &= \mathbb{E}_{R_1} \left[e^{i\omega\eta R_1} \Phi_{\sum_{k=2}^{\infty} R_k^{-1}}(\omega R_1 | R_1) \right] \stackrel{(c)}{=} \mathbb{E}_{R_1} \left[e^{i\omega\eta R_1} \mathbb{E} \left[\prod_{k=2}^{\infty} e^{i\omega R_1 R_k^{-1}} \Big| R_1 \right] \right] \\ &\stackrel{(d)}{=} \mathbb{E}_{R_1} \left[e^{i\omega\eta R_1} \cdot \exp \left(- \int_{r=R_1}^{\infty} (1 - e^{i\omega R_1 r^{-1}}) \lambda(r) dr \right) \right], \end{aligned}$$

where (a) is obtained due to the properties of expectation, and R_1 is the random variable for the distance of the closest BS from the origin, (b) is obtained by using the properties of the characteristic functions and noting that in $\frac{1}{\text{SINR}_{\text{canonical}}} = \frac{\sum_{k=2}^{\infty} R_k^{-1} + \eta}{R_1^{-1}}$, conditioned on R_1 , the term $\frac{\eta}{R_1^{-1}}$ is a constant and hence separates out as $e^{i\omega\eta R_1}$ from the original conditional characteristic function expression in (a), (c) is obtained by rewriting the exponential of summation in the characteristic function term in (b) as a product of exponentials, (d) is obtained by first noting that conditioned on R_1 , the events in the two disjoint regions $[0, R_1]$ and (R_1, ∞) are independent of each other, and hence by the Restriction theorem [26, Page 17], all the points beyond R_1 , represented by the set $\{R_k\}_{k=1}^{\infty}$ can be regarded to be associated with a Poisson point process in 1-D restricted to the region (R_1, ∞) , and with a density function $\lambda(r)$. As a result, now we can apply Campbell's theorem [26, Page 28] to the inner expectation in (c) to obtain (d), which is further simplified to obtain (6).

E. Proof for Theorem 4

Here, we derive the expression for the tail probability of SINR for values greater than or equal to 1. Due to [32, Lemma 1], there exists a unique BS within the 1-D SCS such that $\gamma \geq 1$ holds true. Let the index of this unique BS be i . The expression for the tail probability of SINR is

derived as follows.

$$\begin{aligned}
\mathbb{P}(\{\text{SINR} > \gamma\}) &\stackrel{(a)}{=} \mathbb{P}\left(\left\{\frac{\Psi_i R_i^{-1}}{\sum_{j=1, j \neq i}^{\infty} \Psi_j R_j^{-1} + \eta} > \gamma\right\}\right) \\
&\stackrel{(b)}{=} \mathbb{E}\left[\exp(-\eta\gamma R_i) \prod_{j=1, j \neq i}^{\infty} \exp(-\gamma R_i \Psi_j R_j^{-1})\right] \\
&\stackrel{(c)}{=} \mathbb{E}\left[\exp(-\eta\gamma R_i) \exp\left(-\int_{r=0}^{\infty} \left(1 - \mathbb{E}_{\Psi}\left[e^{-\gamma R_i \Psi r^{-1}}\right]\right) \bar{\lambda}(r) dr\right)\right] \\
&\stackrel{(d)}{=} \mathbb{E}\left[\exp(-\eta\gamma R_i) \exp\left(-\int_{r=0}^{\infty} \left(1 - \frac{1}{1 + \gamma R_i r^{-1}}\right) \bar{\lambda}(r) dr\right)\right],
\end{aligned}$$

where (a) is the expression for the tail probability of SINR of the 1-D SCS with BS density $\bar{\lambda}(r)$ for which $\{R_j\}_{j=1}^{\infty}$ is the set of distances of BSs from the MS and ‘i’ is the index of the unique BS that can satisfy the constraint $\{\text{SINR} > \gamma\}$, (b) is obtained by evaluating the expectation w.r.t. Ψ_i and the expectation operator \mathbb{E} is w.r.t. to all other random variables in (a), (c) is obtained by first conditioning w.r.t. R_i and noting that the Palm distribution of the BSs represented by $\{R_j\}_{j=1, j \neq i}^{\infty}$ given a BS at R_i is still a Poisson point process with density function $\bar{\lambda}(r)$, then applying the Marking theorem [26, Page 55] and Campbell’s theorem [26, Page 28] where Ψ is the unity mean exponential random variable, (d) is obtained by evaluating the expectation in (c), and finally (7) is obtained by simplifying (d).

F. Proof for the Few-BS Approximation Theorem (Theorem 5)

First, using Corollary 4, $\text{SIR}_2 = \frac{KR_1^{-\varepsilon}}{\tilde{P}_I(2)}$, with $\tilde{P}_I(2) = KR_2^{-\varepsilon} \left(1 + \frac{\lambda_0 b_l}{\varepsilon - l} R_2^l\right)$. Next, notice that the event $\{\text{SIR}_2 > \gamma\}$ is equivalent to the joint event $\left\{R_1 \leq R_2, R_1 < \left(\frac{\gamma \tilde{P}_I(2)}{K}\right)^{-\frac{1}{\varepsilon}}\right\}$ and thus, $\mathbb{P}\left(\left\{\frac{C}{I_2} > \gamma\right\}\right) = \mathbb{P}\left(\left\{R_1 \leq \min\left(R_2, \left(\frac{\gamma \tilde{P}_I(2)}{K}\right)^{-\frac{1}{\varepsilon}}\right)\right\}\right)$, where

$$\min\left(R_2, \left(\frac{\gamma \tilde{P}_I(2)}{K}\right)^{-\frac{1}{\varepsilon}}\right) = \begin{cases} \left(\frac{\gamma \tilde{P}_I(2)}{K}\right)^{-\frac{1}{\varepsilon}}, & \gamma \geq 1 \\ \left(\frac{\gamma \tilde{P}_I(2)}{K}\right)^{-\frac{1}{\varepsilon}}, & \gamma < 1, R_2 > \left(\frac{l \times u(\gamma)}{\lambda_0 b_l}\right)^{\frac{1}{l}} \\ R_2, & \gamma < 1, R_2 \leq \left(\frac{l \times u(\gamma)}{\lambda_0 b_l}\right)^{\frac{1}{l}} \end{cases}.$$

Finally, (15) is obtained using the joint p.d.f., $f_{R_1, R_2}(r_1, r_2) = (\lambda_0 b_l)^2 (r_1 r_2)^{l-1} \exp\left(-\frac{\lambda_0 b_l}{l} r_2^l\right)$, $0 \leq r_1 \leq r_2 \leq \infty$, due to the properties of Poisson point processes.

G. Proof for Theorem 6

Let us consider the probability of the event that the interference due to all the BSs beyond the signal BS at a given distance R_1 is below a certain value, say, δ , for the case $\varepsilon = 2$.

$$\begin{aligned}
& \mathbb{P}\left(\left\{\sum_{k=2}^{\infty} R_k^{-2} \leq \delta \mid R_1\right\}\right) = \mathbb{P}\left(\left\{e^{-s \sum_{k=2}^{\infty} R_k^{-2}} \geq e^{-s\delta} \mid R_1\right\}\right) \\
& \stackrel{(a)}{\leq} e^{s\delta} \mathbb{E}\left[e^{-s \sum_{k=2}^{\infty} R_k^{-2}} \mid R_1\right] \stackrel{(b)}{=} e^{s\delta} e^{-\lambda \int_{r=R_1}^{\infty} (1-e^{-sr^{-2}}) 2\pi r dr} \\
& \stackrel{(c)}{=} e^{s\delta} e^{\lambda \int_{r=R_1}^{\infty} \sum_{k=1}^{\infty} \frac{(-sr^{-2})^k}{k!} 2\pi r dr} \\
& = e^{s\delta} e^{-\lambda s 2\pi \cdot \log(r)|_{r=R_1}^{\infty} + \lambda 2\pi \sum_{k=2}^{\infty} \frac{(-s)^k}{k!} \frac{(R_1^{2-k\varepsilon})}{k\varepsilon-2}} \\
& = e^{s\delta} \times 0 \times e^{\alpha(R_1)} = 0,
\end{aligned}$$

where (a) is obtained by applying Markov's inequality, (b) is obtained by applying Campbell's theorem to the homogeneous Poisson point process defined in the 2-D plane beyond R_1 from the origin, (c) is obtained after the Taylor's series expansion of the exponential function in (b), and finally the result is obtained by noting that the exponential of a sum of functions is a product of exponential and by showing that one of the terms in the product is 0 while the others evaluate to a finite number.

As a result,

$$\begin{aligned}
\mathbb{P}(\{SIR > \gamma\}) &= \mathbb{E}_{R_1} \left[\mathbb{P}\left(\left\{\sum_{k=2}^{\infty} R_k^{-\varepsilon} < (\gamma R_1^\varepsilon)^{-1} \mid R_1\right\}\right) \right] \\
&= 0, \quad \forall \gamma \geq 0.
\end{aligned}$$

and hence we have proved the result.

H. Simulation Methods

In this section, the details of simulating the SCS are presented. A single trial in simulating the BS placement for the 1-D SCS with BS density function $\lambda(r)$ in the region of interest which

is a subset of the 1-D plane denoted by S , involves the following steps:

1) Generate a random number M , according to a Poisson distribution with mean $\int_S \lambda(s) ds$, which is the number of BSs to be placed in S for the given trial.

2) *BS placement*: For *homogeneous* 1-D SCS, generate M random numbers according to a uniform distribution in the range of S . If $\lambda(s)$ does not correspond to a *homogeneous* 1-D SCS, if $\lambda_{\max} = \sup_{s \in S} \lambda(s)$, then generate a random number y which is uniformly distributed in the range $[0, \lambda_{\max}]$ and another random number x according to a uniform distribution in the range of S . A BS is placed uniformly at x , only if $y < \lambda_0(x)$. This process is repeated until M BS are placed.

3) Compute the received power at the MS for each BS using the path-loss exponent ε . The fading in the SCS is incorporated by multiplying each of the received powers with i.i.d. random number generated according to the distribution of the fading factor. Finally, SINR at the MS corresponding to this trial, is computed according to (2).

For all the simulations in this paper $T = 100,000$ trials are used unless specified otherwise.

REFERENCES

- [1] T. X. Brown, "Cellular performance bounds via shotgun cellular systems," *IEEE J. Sel. Areas Commun.*, vol. 18, no. 11, pp. 2443–2455, Nov 2000.
- [2] V. Chandrasekhar and J. Andrews, "Uplink capacity and interference avoidance for two-tier femtocell networks," *IEEE Transactions on Wireless Communications*, vol. 8, no. 7, pp. 3498–3509, July 2009.
- [3] J. G. Andrews, N. Jindal, M. Haenggi, R. Berry, S. Jafar, D. Guo, S. Shakkottai, R. W. H. Jr., M. Neely, S. Weber, and A. Yener, "Rethinking information theory for mobile ad hoc networks," *IEEE Communications Magazine*, vol. 46, no. 12, pp. 94–101, December 2008.
- [4] A. M. Hunter, J. G. Andrews, and S. Weber, "Capacity scaling laws for ad hoc networks with spatial diversity," in *Proceedings of the IEEE International Symposium on Information Theory (ISIT)*, Nice, France, June 2007.
- [5] —, "Capacity scaling of ad hoc networks with spatial diversity," *IEEE Transactions on Wireless Communications*, vol. 7, no. 12, pp. 5058–5071, December 2008.
- [6] N. Jindal, J. G. Andrews, and S. Weber, "Energy-limited vs. interference-limited ad hoc network capacity (invited)," in *Proceedings of the 41st Annual Asilomar Conference on Signals, Systems, and Computers*, Pacific Grove, CA, November 2007.
- [7] K. T. Truong, S. Weber, and R. W. Heath, "Transmission capacity of two-way communication in wireless ad hoc networks," in *Proceedings of the International Conference on Communications (ICC)*, Dresden, Germany, June 2009.

- [8] S. Weber, J. G. Andrews, X. Yang, and G. de Veciana, "Transmission capacity of CDMA ad hoc networks employing successive interference cancellation," in *Proceedings of the 47th annual IEEE Global Telecommunications Conference (Globecom)*, Dallas, TX, November 2004.
- [9] —, "Wireless ad hoc networks with successive interference cancellation," in *Proceedings of the 43rd annual Allerton conference on communication, control, and computing*, Monticello, IL, September 2005.
- [10] S. Weber and J. G. Andrews, "A stochastic geometry approach to wideband ad hoc networks with channel variations," in *Proceedings of the Second Workshop on Spatial Stochastic Models for Wireless Networks (SPASWIN)*, Boston, MA, April 2006.
- [11] —, "Transmission capacity of wireless ad hoc networks with channel variations," in *Proceedings of the 40th Annual Asilomar Conference on Signals, Systems, and Computers*, Pacific Grove, CA, October 2006.
- [12] S. Weber, X. Yang, G. de Veciana, and J. Andrews, "Transmission capacity of CDMA ad-hoc networks," in *Spread Spectrum Techniques and Applications, 2004 IEEE Eighth International Symposium on*, 2004, pp. 245–249.
- [13] S. Weber, X. Yang, J. G. Andrews, and G. de Veciana, "Transmission capacity of wireless ad hoc networks with outage constraints," *IEEE Transactions on Information Theory*, vol. 51, no. 12, pp. 4091–4102, December 2005.
- [14] J. Wildman, D. Hamel, R. Measel, D. Oakum, S. Weber, and M. Kam, "Performance and scaling of wireless ad hoc IPv6 stateless address autoconfiguration under mobile gateways," in *Proceedings of the Military Communications Conference (MILCOM)*, Orlando, FL, October 2007.
- [15] P. Madhusudhanan, J. G. Restrepo, Y. Liu, T. X. Brown, and K. Baker, "Stochastic ordering based carrier-to-interference ratio analysis for the shotgun cellular systems," *Wireless Communications Letters, IEEE*, vol. PP, no. 99, pp. 1–4, 2012.
- [16] —, "Modeling of Interference from Cooperative Cognitive Radios for Low Power Primary Users," in *IEEE Globecom 2010 Wireless Communications Symposium*, 2010, pp. 1–6.
- [17] —, "Multi-tier network performance analysis using a shotgun cellular system," in *IEEE Globecom 2011 Wireless Communications Symposium*, Dec. 2011, pp. 1–6.
- [18] P. Madhusudhanan, J. G. Restrepo, Y. Liu, and T. X. Brown, "Downlink coverage analysis in a heterogeneous cellular network," *CoRR*, 2012. [Online]. Available: <http://arxiv.org/abs/1206.4723>
- [19] S. Weber, J. G. Andrews, and N. Jindal, "Throughput and transmission capacity of ad hoc networks with channel state information," in *Proceedings of the 44th Annual Allerton Conference on Communication, Control, and Computing*, Monticello, IL, September 2006.
- [20] S. Weber, X. Yang, G. de Veciana, and J. G. Andrews, "Transmission capacity of CDMA ad-hoc networks," in *Proceedings of the 8th IEEE International Symposium on Spread Spectrum Techniques and Applications (ISSSTA)*, Sydney, Australia, August 2004.
- [21] J. G. Andrews, S. Weber, and M. Haenggi, "Ad hoc networks: to spread or not to spread?" *IEEE Communications Magazine*, vol. 45, no. 12, pp. 84–91, December 2007.
- [22] N. Jindal, S. Weber, and J. G. Andrews, "Fractional power control for decentralized wireless networks," *IEEE Transactions on Wireless Communications*, vol. 7, no. 12, pp. 5482–5492, December 2008.
- [23] N. Jindal, J. G. Andrews, and S. Weber, "Bandwidth partitioning in decentralized wireless networks," *IEEE Transactions on Wireless Communications*, vol. 7, no. 12, pp. 5408–5419, December 2008.

- [24] H. Takagi and L. Kleinrock, "Optimal transmission ranges for randomly distributed packet radio terminals," *IEEE Transactions on Communications*, vol. 32, no. 3, pp. 246–257, Mar 1984.
- [25] M. Zorzi and S. Pupolin, "Outage probability in multiple access packet radio networks in the presence of fading," *IEEE Transactions on Vehicular Technology*, vol. 43, no. 3, pp. 604–610, Aug 1994.
- [26] J. F. C. Kingman, *Poisson Processes (Oxford Studies in Probability)*. Oxford University Press, USA, January 1993.
- [27] S. M. Ross, *Stochastic Processes*. John Wiley & Sons, Inc., 1983.
- [28] M. Shaked and J. G. Shanthikumar, *Stochastic Orders*, ser. Springer Series in Statistics. Springer, 2007.
- [29] —, *Stochastic Orders and Their Applications (Probability and Mathematical Statistics)*. Academic press, 1994.
- [30] A. M. Mathai and H. J. Haubold, *Special Functions for Applied Scientists*. Springer, March 2008.
- [31] P. Xia, V. Chandrasekhar, and J. Andrews, "Open vs. closed access femtocells in the uplink," *Wireless Communications, IEEE Transactions on*, vol. 9, no. 12, pp. 3798–3809, 2010.
- [32] H. Dhillon, R. Ganti, and J. Andrews, "Load-aware modeling and analysis of heterogeneous cellular networks," *CoRR*, vol. abs/1204.1091, 2012. [Online]. Available: <http://arxiv.org/abs/1204.1091>
- [33] H. S. Dhillon, R. K. Ganti, F. Baccelli, and J. G. Andrews, "Coverage and ergodic rate in K-tier downlink heterogeneous cellular networks," in *49th Annual Allerton Conference on Communication, Control, and Computing (Allerton)*, 2011, sept. 2011, pp. 1627–1632.
- [34] H. Dhillon, R. Ganti, and J. Andrews, "A tractable framework for coverage and outage in heterogeneous cellular networks," in *Information Theory and Applications Workshop (ITA)*, 2011, feb. 2011, pp. 1–6.
- [35] H.-S. Jo, Y. J. Sang, P. Xia, and J. G. Andrews, "Heterogeneous cellular networks with flexible cell association: A comprehensive downlink sinr analysis," *CoRR*, vol. abs/1107.3602, 2011. [Online]. Available: <http://arxiv.org/abs/1107.3602>
- [36] S. Mukherjee, "Distribution of downlink SINR in heterogeneous cellular networks," *IEEE Journal on Selected Areas in Communications*, vol. 30, no. 3, pp. 575–585, april 2012.
- [37] —, "Downlink SINR distribution in a heterogeneous cellular wireless network with biased cell association," in *IEEE ICC 2012 - 1st International Workshop on Small Cell Wireless Networks*, 2012.